

Progressive Dysmorphia of Retinal Pigment Epithelium in Age-Related Macular Degeneration Investigated by Fluorescence Lifetime Imaging

Martin Hammer,^{1,3} Juliane Jakob-Girbig,¹ Linda Schwanengel,¹ Christine A. Curcio,² Somar Hasan,¹ Daniel Meller,¹ and Rowena Schultz¹

¹Department of Ophthalmology, University Hospital Jena, Jena, Germany

²Department of Ophthalmology and Visual Sciences, School of Medicine, University of Alabama at Birmingham, Birmingham, Alabama, United States

³Center for Medical Optics and Photonics, Univ. of Jena, Jena, Germany

Correspondence: Martin Hammer, University Hospital Jena, Department of Ophthalmology, Am Klinikum 1, 07747 Jena, Germany; martin.hammer@med.uni-jena.de.

Received: April 21, 2021

Accepted: August 9, 2021

Published: September 7, 2021

Citation: Hammer M, Jakob-Girbig J, Schwanengel L, et al. Progressive dysmorphia of retinal pigment epithelium in age-related macular degeneration investigated by fluorescence lifetime imaging. *Invest Ophthalmol Vis Sci.* 2021;62(12):2. <https://doi.org/10.1167/iovs.62.12.2>

PURPOSE. The purpose of this study was to observe changes of the retinal pigment epithelium (RPE) on the transition from dysmorphia to atrophy in age-related macular degeneration (AMD) by fluorescence lifetime imaging ophthalmoscopy (FLIO).

METHODS. Multimodal imaging including color fundus photography (CFP), optical coherence tomography (OCT), fundus autofluorescence (FAF) imaging, and FLIO was performed in 40 eyes of 37 patients with intermediate AMD and no evidence for geographic atrophy or macular neovascularization (mean age = 74.2 ± 7.0 years). Twenty-three eyes were followed for 28.3 ± 18.3 months. Seven eyes had a second follow-up after 46.6 ± 9.0 months. Thickened RPE on OCT, hyperpigmentation on CFP, hyper-reflective foci (HRF) on OCT, attributed to single or clustered intraretinal RPE, were identified. Fluorescence lifetimes in two spectral channels (short-wavelength spectral channel [SSC] = 500–560 nm, long-wavelength spectral channel [LSC] = 560–720 nm) as well as emission spectrum intensity ratio (ESIR) of the lesions were measured by FLIO.

RESULTS. As hyperpigmented areas form and RPE migrates into the retina, FAF lifetimes lengthen and ESIR of RPE cells increase. Thickened RPE showed lifetimes of 256 ± 49 ps (SSC) and 336 ± 35 ps (LSC) and an ESIR of 0.552 ± 0.079 . For hyperpigmentation, these values were 317 ± 68 ps ($p < 0.001$), 377 ± 56 ps ($P < 0.001$), and 0.609 ± 0.081 ($P = 0.001$), respectively, and for HRF 337 ± 79 ps ($P < 0.001$), 414 ± 50 ps ($P < 0.001$), and 0.654 ± 0.075 ($P < 0.001$).

CONCLUSIONS. In the process of RPE degeneration, comprising different steps of dysmorphia, hyperpigmentation, and migration, lengthening of FAF lifetimes and a hypsochromic shift of emission spectra can be observed by FLIO. Thus, FLIO might provide early biomarkers for AMD progression and contribute to our understanding of RPE pathology.

Keywords: age-related macular degeneration (AMD), retinal pigment epithelium (RPE), fundus autofluorescence (FAF), fluorescence lifetime, fluorescence spectra, atrophy, migration

Although age-related macular degeneration (AMD) is a multifactorial disease, the end stage of non-neovascular AMD includes atrophy of the retinal pigment epithelium (RPE). This is seen as geographic atrophy (GA) in color fundus photography (CFP) and is incorporated into complete RPE and outer retinal atrophy (cRORA) in optical coherence tomography (OCT).¹ Consequently, RPE alteration, seen in CFP or OCT, is a risk factor for disease progression.^{2–5} Histopathology as well as clinical imaging revealed multiple morphologically distinct pathways to atrophy, mainly intraretinal migration and shedding of organelles into underlying basal laminar deposits (BLamDs).^{6,7} The best studied pathway involves RPE cells detaching from the

RPE basal lamina (BL) and subsequently migrating into the retina, where they appear as hyper-reflective foci (HRF) in OCT.^{5,8–10} In a post hoc analysis of a standardized imaging dataset from a prospective clinical trial, HRF were found to confer risk for RPE atrophy with a 2 year odds ratio of 5.2.¹¹

Due to its accumulation of lipofuscin and melanolipofuscin, RPE contributes the strongest fluorescence emission in fundus autofluorescence imaging (FAF).^{12–17} High resolution microscopy revealed distinct autofluorescent organelles¹⁸ and spectrally resolved microscopy uncovered emission spectra specific for RPE fluorophores and for sub-RPE tissues.¹⁹ Hyperautofluorescence in FAF was studied as a marker of AMD progression and GA growth clinically^{20–24}

as well as in histopathology.²⁵ Furthermore, hyperpigmentation in CFP is associated with hyperautofluorescence in FAF.^{16,17}

Fluorescence lifetime imaging ophthalmoscopy (FLIO) is a technique extending FAF imaging to the measurement of fluorescence lifetimes.^{26–28} Measuring the average time (in the order of picoseconds) a fluorescent molecule remains in an excited electronic state after excitation by a short laser pulse, fluorescence lifetime imaging characterizes the molecule, and its embedding matrix. In clinical FLIO imaging, however, a variety of fluorophores can contribute to the signal. As it is impossible to resolve all molecules from the fluorescence decay signal, these measurements cannot directly address single molecules but characterize the overall state of tissue, comprising all retinal layers, at each pixel in the image.²⁹ A general prolongation of FAF lifetimes^{30,31} as well as further prolongation with disease progression was found in AMD.³² Specifically, hyperpigmented areas in CFP exhibited longer FAF lifetimes and shorter emission wavelengths than the surrounding less affected areas in the fundus.³³

In the current retrospective study, we used multimodal imaging to investigate the natural history of drusen-associated RPE dysmorphia as defined in CFP and OCT, with the expectation that these cells are abnormal and thus would exhibit distinctive signals in FAF and FLIO. In this study, dysmorphic RPE atop drusenoid RPE detachment (PED), hyperpigmentation, and migrated RPE were examined separately in order to observe FAF lifetime changes and identify AMD progression markers seen in FLIO. A second pathway to RPE atrophy, related to subretinal drusenoid deposits, was not considered here.

METHODS

Subjects and Procedures

In this retrospective study, patients with AMD, which was non-neovascular at the time of inclusion, seen at the University Hospital Jena, Department of Ophthalmology, between April 2014 and January 2021 were enrolled. Exclusion criteria were the presence of GA or macular neovascularization at the baseline visit, other retinal retina-involving pathologies, such as diabetic retinopathy, glaucoma, hypertensive retinopathy, retinal vascular occlusion, central serous chorioretinopathy, macular telangiectasia 2, Stargardt disease, retinitis pigmentosa, macular holes, and retinal detachment. Patients were also excluded in case of mature cataract preventing high quality fundus imaging.

The study was approved by the ethics committee of the University Hospital Jena and adhered to the tenets of the Declaration of Helsinki. All participants gave written informed consent prior to study inclusion and underwent a full ophthalmologic examination including best corrected visual acuity, OCT (Cirrus-OCT; Carl-Zeiss Meditec AG, Jena, Germany) and CFP (Visucam; Carl-Zeiss Meditec AG, Jena, Germany). Pupils were dilated using tropicamide (Mydraticum Stulln; Pharma Stulln GmbH, Nabburg, Germany) and phenylephrine-hydrochloride (Neosynephrin-POS 5%; Ursapharm GmbH, Saarbrücken, Germany). After pupil dilation, patients underwent imaging with FLIO, OCT (21-lines HD as well as 512 × 128 pixel macula cube scans), and CFP. No sodium fluorescein was administered topically or intravenously prior to FLIO investigation.

FLIO Imaging and Data Analysis

Basic principles and laser safety of FLIO are described elsewhere.^{34–36} FLIO image capture is based on a picosecond laser diode coupled with a laser scanning ophthalmoscope (Spectralis; Heidelberg Engineering, Heidelberg, Germany), exciting retinal autofluorescence at 473 nm with a repetition rate of 80 Mhz. Fluorescence photons were detected by time-correlated single photon counting (SPC-150; Becker & Hickl GmbH, Berlin, Germany) in short-wavelength (short spectral channel [SSC] = 498–560 nm) and long-wavelength (long spectral channel [LSC] = 560–720 nm) spectral channel. FLIO provides 30 degrees field images with a frame rate of 9 frames per second and a resolution of 256 × 256 pixels. Photon histograms over time, describing the autofluorescence decay, were least-square fitted with a series of 3 exponential functions using the software SPCImage 6.0 (Becker & Hickl GmbH). The amplitude-weighted mean decay time τ_m is called FAF lifetime and used for subsequent analysis. The resulting image is color-coded, depicting short lifetimes in red and long lifetimes in blue color. In addition, the ratio of photon counts (autofluorescence intensity) in SSC and LSC was calculated per pixel, which is denoted as the emission spectrum intensity ratio (ESIR; previously called spectral ratio).

The software FLIMX, which is documented and freely available for download under an open-source Berkeley Software Distribution (BSD) license (<http://www.flimx.de>),³⁷ was used for the manual selection of lesions as regions of interest (ROI). As there was no automatic image registration available for CFP, OCT, and FLIO, the registration was done manually to make sure that we address the same lesions in all imaging modalities. Mean FAF lifetimes and ESIR per pixel were averaged over all pixels of the ROI as well as the environment of the ROI, a 105- μ m wide area, which was 35 μ m distant to the ROI.

From previous literature, several imaging indicators of dysmorphic RPE and its underlying BL can be assembled for use in reference to FLIO. The RPE and the RPE-BL are best thought of as separate from an underlying three-layer Bruch's membrane.^{38,39} In OCT, a thickening of the RPE-BL band can be observed especially over drusen and drusenoid pigment epithelial detachment (PED).⁴⁰ Thickening precedes the appearance of HRF directly above in the overlying retina but thickening may or may not still be present if and when HRF appears. In non-neovascular AMD, HRF have been directly correlated with nucleated cells containing RPE organelles at the same qualitative abundance as cells in the intact RPE layer^{6,40}; in neovascular AMD HRF also includes lipid-filled cells not resembling RPE.^{41,42} Hyperpigmentation in CFP is a nonspecific term that encompasses several possibilities, including proliferation (cell division) of RPE cells, rounding or stacking individual RPE cells, and increased size or concentration of melanin-containing organelles (melanosomes and melanolipofuscin), all of which may increase pathlength of light through light-absorbing melanin protein.⁴³ Thus, hyperpigmentation in CFP can be associated with thickened RPE-BL or HRF in OCT. Thickening of RPE-BL, however, also can occur without hyperpigmentation.

Two reviewers (authors J.J.G. and M.H.), masked to the lifetimes, marked hyperautofluorescent areas in FAF (SSC or LSC) and graded them according to OCT and CFP features: OCT was checked for the presence of drusen or drusenoid PED (smallest diameter > 350 μ m),⁴⁴

thickening of the RPE-BL band, and the presence or absence of HRF anterior to the ellipsoid zone.⁴⁵ CFP was checked for the presence or absence of hyperpigmentation. This way, we found three lesion entities consistent with the histologic findings described above: (i) a thickened RPE-BL band atop drusenoid PED with no hyperpigmentation in CFP, (ii) hyperpigmentation associated with thickened RPE-BL but no HRF, and (iii) HRF independent from the thickness of the underlying RPE-BL which was hyperpigmented.

Lesions were excluded if the reviewers graded differently. To exclude hyperautofluorescent drusen from the analysis, areas that were not clearly thickened in OCT and hyperpigmented in CFP were excluded. In addition, areas with incipient atrophy were excluded. Lesions in the fovea (central 400 μm in diameter) were excluded as well because of FLIO signal from macular xanthophyll pigment. Acquired vitelliform lesions were also excluded. Grading was done independently for each patient visit without reference to the prior visit.

Statistics

FAF lifetimes and ESIR of lesions and their environment were compared by paired *t*-test. Data for groups of lesions (thickened RPE-BL, hyperpigmentation, and HRF) was compared using ANOVA with post hoc Bonferroni test compensating for multiple testing. For this test, each lesion entity was included at baseline. The correlation of the follow-up time with the changes of lifetimes and ESIR from baseline to follow-up was tested.

RESULTS

Forty eyes of 37 patients (mean age = 74.2±7.0 years) were included. Twenty-four eyes (60%) were pseudophakic. Thirty eyes of 25 patients had a follow-up of 28.3 ± 18.3 months. Twelve of these eyes had a second follow-up (mean follow-up time 46.6 ± 9.0 months after baseline). Study patient demographics and lesion fate are given in Table 1. At baseline, we found 58 areas of thickened RPE atop PED on OCT, 38 areas of hyperpigmentation on CFP without PED on OCT, and 126 HRF. We observed the disappearance of 9 PEDs (6 at first and 3 at second follow-up) and 15 HRF at first follow-up. Four spots of hyperpigmentation turned to HRF at follow-up. Over follow-up, we found 11 newly appearing PEDs, 7 new spots of hyperpigmentation (3 over drusen and 4 over PED), and 28 new HRF (6 over drusen and 22 over

recent or collapsed PED). At first follow-up, 5 out of 30 eyes had a central cRORA, one a paracentral cRORA, one an outer retinal atrophy, and 3 a macular neovascularization (MNV). At the second follow-up, we found one more central and one more parafoveal (inner ring of the ERTDRS-grid) cRORA as well as one more MNV.

Hyperpigmentation and HRF have strong FAF with long lifetimes whereas thickened RPE on top of PED shows diffuse hyperfluorescence with short lifetimes. A typical example is shown in Fig. 1. This patient was imaged at baseline and at two follow-up visits 24 and 52 months later. The natural history of PED is exemplified in two OCT sections. Superior to the macula we see a PED with hyperpigmentation at baseline. Its growth over 24 months is associated with the appearance of HRF (see Fig 1e) showing strong focal hyperfluorescence with long lifetimes (at white arrowheads). At month 52, the PED is partly collapsed and partly denuded of RPE. Atrophy is seen by the penetration of laser light into the choroid in OCT (see Fig 1f) and a hypofluorescence with long lifetimes in LSC (see Figs. 1p, 1v). Interestingly, this incipient atrophy does not show hypofluorescence but already long lifetimes in SSC. Whereas we hardly see RPE attached to the still-elevated persistent BLamD (red arrowhead in Fig. 1f), HRF remaining in the retina (see Fig. 1f), and can contribute to the long lifetime fluorescence. Inferior to the macula, we see also growth of PED, which becomes hyperautofluorescent at month 24 (see Figs. 1l, 1o, black arrowhead). In contrast to hyperpigmentation and HRF, PED have short FAF lifetimes. At month 52, we found these PEDs collapsed leaving large HRF with long lifetimes again (black arrowheads in Figs. 1c, 1i, 1m, 1p, 1s, 1v). Finally, at month 52, we see one very small HRF (purple arrowhead in Figs. 1c, 1j, 1m, 1p, 1s, 1v), which is hardly discernible in CFP. FLIO, however, clearly shows that this lesion has a long FAF lifetime.

Whereas intraretinal HRF (i.e. internal to the ellipsoid zone) always show long lifetimes, in hyperpigmentation associated with focal thickening of the RPE-BL band we found a transition from short to long lifetimes. Figure 2 shows an example (arrowheads point to hyperpigmented spots with various FAF lifetimes). At hyperpigmentation (Fig. 3, arrowhead), we observed a change from hyperfluorescence with initially short lifetime to long lifetime upon the appearance of HRF with no PED 35 months later. However, long lifetimes are also seen before the advent of atrophy in the absence of HRF. Fig. 4 shows a patient at baseline and 21 months later. The white arrowheads point to thickened RPE showing short lifetime, whereas long lifetimes also were

TABLE 1. Patient Demographics and Fate of RPE Lesions

Patient Information	Baseline	Follow Up 1	Follow Up 2
N (patients)	37 (100%)	25 (68%)	11 (30%)
Female	23 (62%)	14 (56%)	5 (45%)
Male	14 (38%)	11 (44%)	6 (55%)
Age (years, mean ± SD)	74.2 ± 7.0	74.0 ± 6.3	70.8 ± 4.5
N (eyes)	40 (100%)	30 (30%)	12 (30%)
Eyes progressed to MNV		3 (10%)	4 (33%)
Eyes progressed to atrophy		6 (20%)	8 (67%)
RPE lesions	N	gain(+)/loss(-)	gain(+)/loss(-)
Thickened atop PED	58 (100%)	+5 (9%)/-6 (10%)	+11 (19%)/-9 (16%)
Hyperpigmentation	38 (100%)	+2 (5%)/-4 (11%)	+7 (18%)/-4 (11%)
HRF	126 (100%)	+15 (12%)/-15 (12%)	+28 (22%)/-15 (12%)

Percentages of number of eyes at follow ups refer to that at baseline. Percentages of female subjects, male subjects, and AMD progression refer to the number of subjects at the respective visit. Percentages of gain and loss of lesions refer to the number at baseline.

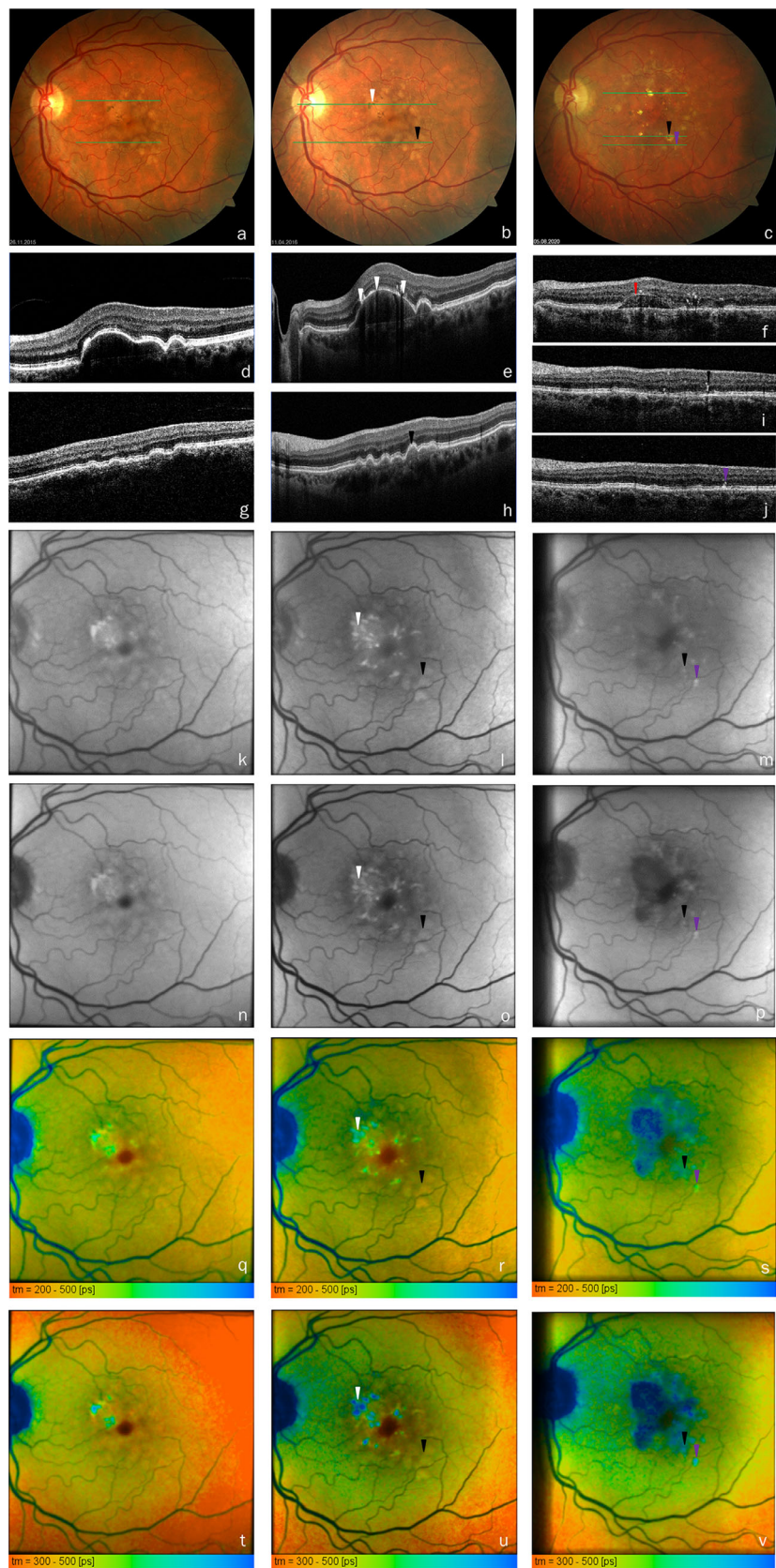


FIGURE 1. Natural history of a PED with RPE migration. (A–C) CFP, (D–J) OCT, (K–M) FAF SSC, (N–P) FAF LSC, (Q–S) FLIO SSC, and (T–V) FLIO LSC of a 64-year-old patient at baseline (left column: A, D, G, K, N, Q, and T), 24 months (middle column: B, E, H, L, O, R, and U) and 52 months follow-up (right column: C, F, I, J, M, P, S, and T). Green lines in A to C show the localization of OCT scans. *White arrowheads*: HRF that correspond to hyperpigmentation on CFP. *Red arrowhead*: BLamD that persists after death or migration of RPE. *Black arrowheads*: Growth of PED at months 24 leaving migrated RPE at month 52. *Purple arrowhead*: Migrated RPE with HRF, no history of PED at this point, but clearly prolonged lifetimes in FLIO.



FIGURE 2. RPE cells detaching from the RPE layer. (A) CFP, (B, C) OCT (scans were tilted to display them horizontally, thus shadows of the hyperpigmentations are obliquely oriented), (D) FAF SSC, (E) FAF LSC, (F) FLIO SSC, and (G) FLIO LSC of an 81-year-old patient. *White arrowheads* show corresponding hyperpigmentation **A**, activated RPE cells **B** and **C**, iso- and hyper-FAF **D** and **E**, and lengthening lifetimes **F** and **G**.

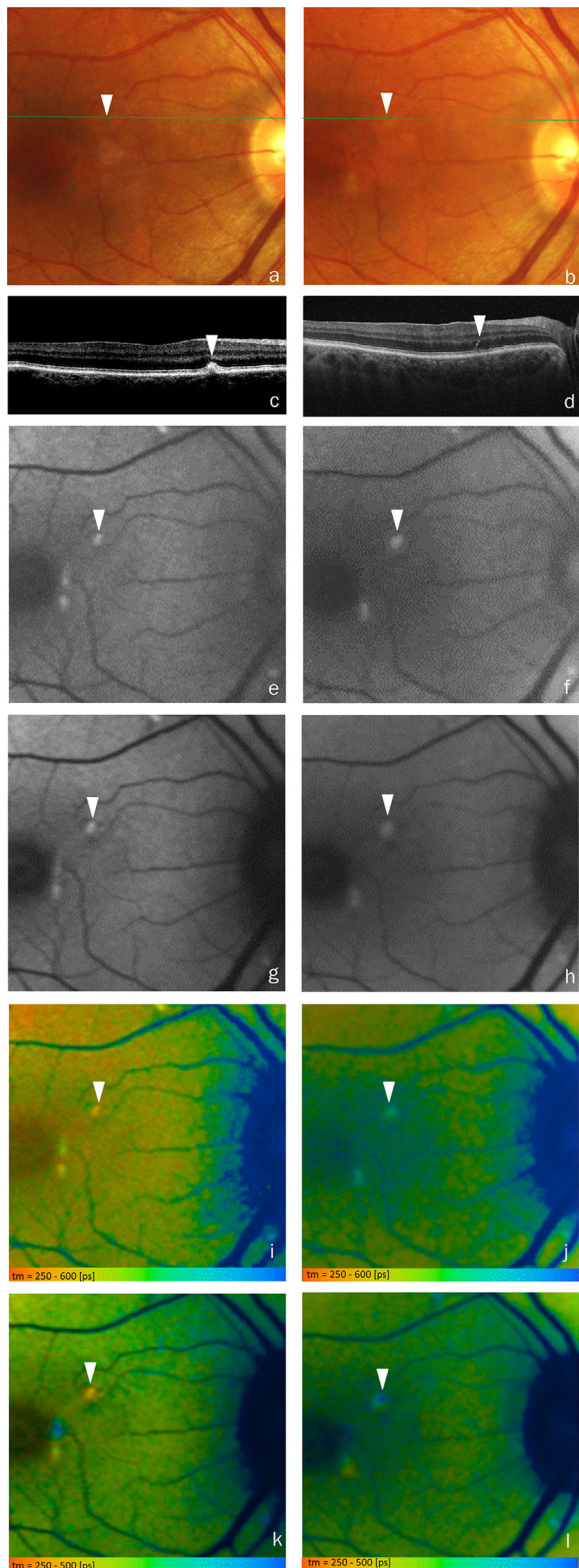


FIGURE 3. Change of FAF lifetime of RPE in the conversion to HRF. (A, B) CFP, (C, D) OCT, (E, F) FAF SSC, (G, H) FAF LSC, (I, J) FLIO SSC, and (K, L) FLIO LSC of a 74-year-old patient at baseline (left column: A, C, E, G, I, and K) and 35 months follow-up (right column: B, D, F, H, J, and L). The *white arrowhead* indicates a hyperpigmentation with short FAF lifetime atop a druse. At follow-up, the druse was resorbed (no PED) and RPE changed to long FAF lifetime upon conversion to HRF. It shows spatial heterogeneity in the changing of lifetimes.

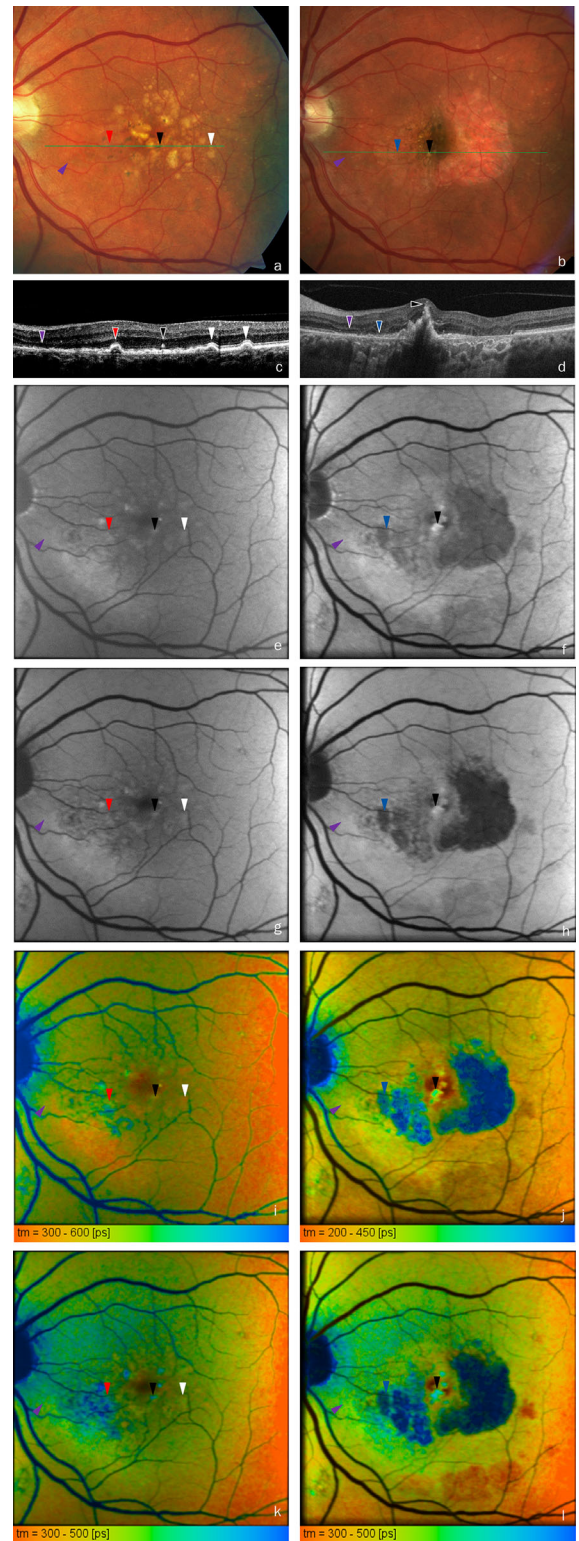


FIGURE 4. Different lifetimes are found in activated and migrated RPE as well as outer retinal atrophy and cRORA. (A, B) CFP, (C, D) OCT, (E, F) FAF SSC, (G, H) FAF LSC, (I, J) FLIO SSC, and (K, L) FLIO LSC of a 69-year-old patient at baseline (left column: A, C, E, G, I, and K) and 21 months (right column: B, D, F, H, J, and L) follow-up. Activated RPE atop PED (*white arrowheads*) shows short FAF lifetime, however, also transition to long lifetime is seen (*red arrowheads*). Furthermore, migrated RPE (*black arrowhead*), outer retinal atrophy (*purple arrowhead*), and cRORA (*blue arrowhead*) are seen.

TABLE 2. RPE Lesions at Baseline

		Lesion	Vicinity	Mean Difference	P For Difference
Thickened RPE-BL band	τ_m SSC	256 ± 49 ps	261 ± 56 ps	-5.0 ± 9.0 ps	<0.001
	τ_m LSC	336 ± 35 ps	338 ± 34 ps	-1.1 ± 5.5 ps	0.118
	ESIR	0.552 ± 0.079	0.547 ± 0.088	0.005 ± 0.022	0.087
Hyperpigmentation	τ_m SSC	317 ± 68 ps	310 ± 69 ps	7.0 ± 22.6 ps	0.063
	τ_m LSC	377 ± 56 ps	365 ± 50 ps	11.9 ± 15.5 ps	<0.001
	ESIR	0.609 ± 0.081	0.600 ± 0.080	0.010 ± 0.035	0.096
HRF	τ_m SSC	337 ± 79 ps	324 ± 87 ps	13.6 ± 19.4 ps	<0.001
	τ_m LSC	414 ± 50 ps	389 ± 46 ps	24.8 ± 18.1 ps	<0.001
	ESIR	0.654 ± 0.075	0.643 ± 0.072	0.011 ± 0.032	<0.001

FAF lifetimes and ESIR (mean ± standard deviation) of RPE lesions at the lesion and in its vicinity, as well as the mean of individual differences (lesion - vicinity) of these measures with *P* values from paired *t*-test.

found on PED (red arrowhead). Furthermore, HRF (black arrowhead), outer retinal atrophy (purple arrowhead), and cRORA (blue arrowhead) are seen.

The average FAF lifetimes and ESIR, found for thickened RPE, hyperpigmentation, and HRF, are given in Table 2 and shown as boxplots in Fig. 5. HRFs have significantly longer lifetimes in both spectral channels and emit at shorter wavelengths (higher ESIR) than their respective environments. For hyperpigmentation, we found longer lifetimes in LSC only. Thickened RPE atop PED exhibited significantly shorter lifetimes than in the vicinity of these lesions in SSC. A comparison of the lesion types showed significantly longer FAF lifetimes for the hyperpigmentation and HRF than for thickened RPE (both spectral channels $P < 0.001$). They were significantly longer for HRF than for hyperpigmentation in LSC ($P < 0.001$); in SSC the difference was nonsignificant ($P = 0.374$). The ESIR significantly increased from thickened RPE to hyperpigmentation to HRF, and the mean values were significantly different for all groups ($P \leq 0.007$). No correlation was found between the change of FAF lifetimes or ESIR of any lesion type and the time to follow-up.

DISCUSSION

RPE dysmorphia suggestive of pathologic activation is a key symptom of AMD. Hyperpigmentation and HRF are known indicators for the risk of AMD progression to cRORA in CFP and OCT, respectively.^{4,46} Shedding cells drop granule aggregates into the underlying BLamD.⁶ Subducted cells containing RPE organelles are found between the RPE-BL and the inner collagenous layer of Bruch's membrane,⁴⁷ and acquired vitelliform lesions may result from the expulsion of organelles.^{40,48} Some of these alterations can be seen in CFP as hyper- or hypopigmentation due to modulation of light absorptive melanin and RPE thickening in OCT. Clinicopathologic correlation revealed that in non-neovascular AMD HRF represent single and clustered RPE cells that detached from their BL and migrated into the retina.⁴⁸

The principal result of our study is the finding of a transition from short to long lifetimes, along with a hypsochromic shift of the emission spectrum, in the compromised RPE. Whereas hyperpigmentation shows longer lifetimes than its environment only in LSC, a switch to long lifetimes in both channels is seen after cells activate and detach from the RPE layer and migrate beyond the ellipsoid zone. We could not completely elucidate at which point in the transition of the RPE cells from activation to atrophy this switch

happens. Figures 2 to 4 indicate a gradual change of lifetimes not only for cells sloughed into the subretinal space, but also for in-layer cells still attached to Bruch's membrane. Whether these cells were dissociated and what role BLamD³⁹ plays if any remains to be determined by techniques providing higher resolution.

Furthermore, it is not clear yet whether the focal prolongation of lifetimes at hyperpigmentation and HRF is associated to a general prolongation of lifetimes in patients with AMD in an annulus corresponding to the outer ring of the Early Treatment of Diabetic Retinopathy Study grid (inner diameter 3 mm and outer diameter 6 mm, centered on the fovea).³⁰

Hyperpigmentation as well as HRF were associated with hyper-FAF. This could be explained by the fact that a monolayer RPE layer has been replaced by stacking or clumping of cells. However, the prolongation of FAF lifetimes as well as the shift of the emission spectrum also indicate a change in fluorophore composition or intracellular environment. An alternative explanation of the hyperautofluorescence of hyperpigmentation and HRF with long lifetimes would be fluorescence from collagen IV²⁹ accumulated in BLamD.^{39,49} However, HRF represent RPE cells migrated off their BL and the long lifetimes seem to be restricted to the spots of HRF. Thus, collagen IV in BLamD has to be questioned as a source of this particular long lifetime fluorescence.

In agreement with Sauer et al.,⁵⁰ thickened RPE atop drusenoid PED showed increased FAF intensity with shortened lifetime in SSC. Although it can be questioned whether a statistically significant 5 ps shortening of FAF lifetime has a biological relevance, this might have various explanations. First, if fluorophore composition is altered as well, the alteration differs from that in hyperpigmentation and HRF. Second, we might see fluorophores other than those in lipofuscin and melanolipofuscin, as their emission maximum is in the LSC,^{51,52} but FAF lifetime shortening is seen in SSC. Third, the additional fluorescence could originate from the drusenoid PED and not from the RPE. This, however, is questionable as hyperfluorescent drusen tend to have longer lifetimes.⁵³ This was more clearly seen for drusen in areas of GA (i.e. not covered by RPE⁵⁴) as well as in histopathology.⁵⁵

Taken together, FLIO, in combination with other imaging modalities, suggests the following natural history of disease progression from PED to atrophy. First, RPE cells were thickened and hyperfluorescence. In this state, we see a growth of the PED, indicating a higher rate of basal deposition of material by the cells or an increased resistance for clearance through Bruch's membrane and choriocapillaris^{56,57} or

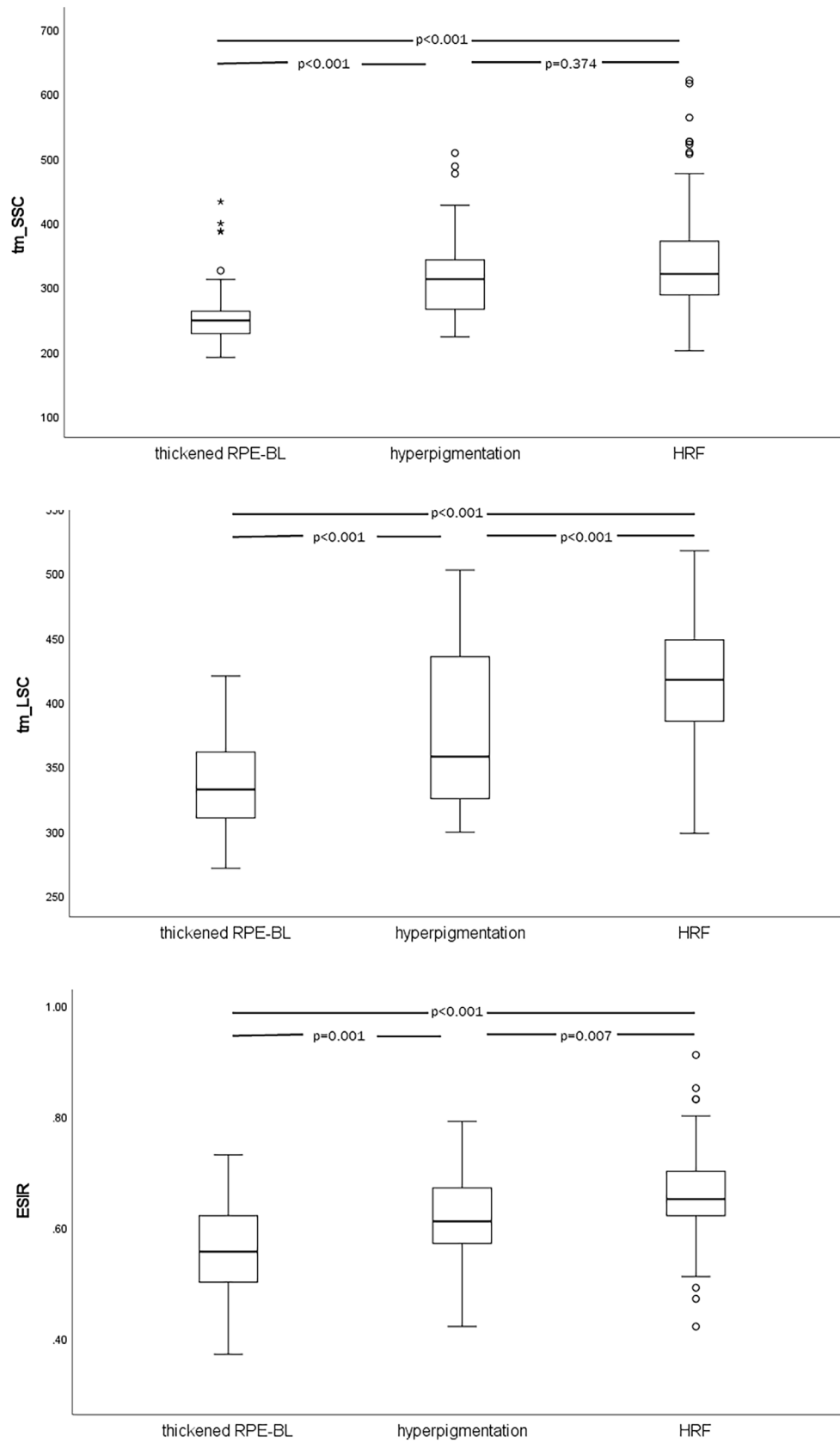


FIGURE 5. FAF lifetimes and ESIR. Boxplots of FAF lifetimes (top: SSC, middle: LSC) and ESIR (bottom) for activated RPE, hyperpigmentations, and migrated RPE. The P values are from post hoc Bonferroni test after ANOVA.

both. Subsequently, hyperpigmentation is observed, which was often found to be associated to RPE cells sloughing from the layer and migration of the cells into the retina in histology.^{5,8,10,40,48,58-62} As clinical imaging and histology revealed RPE migration toward retinal vessels⁴⁰ as along Bruch's membrane (subducted cells),⁶ we may speculate that deficiency in oxygen and/or nutrients, especially glucose,⁶³ is a driving force for migration. Migration or death of some cells leave others attached to Bruch's membrane but dissociated. Finally, death of RPE together with that of the photoreceptors results in cRORA. Whereas dissociated and subducted cells are known from histology,^{47,64} they were not seen in our investigation due to the limited resolution of OCT and FLIO.

Usually, FAF is associated to lipofuscin and melanolipofuscin. However, both contain mixtures of different compounds with different fluorescence properties. Eldred and Katz described 10 fluorescent species and recorded their spectra.⁵¹ A change of the mix of different RPE granules over age is reported and Ach et al. hypothesize that lipofuscin and melanolipofuscin granules can undergo formation, maturation, and deletion in a dynamic process.¹⁸ Thus, a change of the fluorophore composition of RPE, either degenerating or rescuing itself by migration, is not unlikely. Different phenotypes of RPE granules, associated with hypo- or hyperfluorescence of the cells, are described.^{65,66} This further hints at the possible changes of FAF properties in the course of cellular atrophy, however, a direct comparison is difficult. The prior authors^{65,66} did not measure FAF lifetimes or spectra and the resolution in our investigation is insufficient to resolve single granules. High-resolution microscopy of RPE flat mounts revealed degranulation and granule aggregation in AMD donor eyes.¹⁸ According to the authors, this may explain the clinical observation of reduced FAF in aged eyes (above 70 years). The RPE alterations found in our study, however, show hyperfluorescence. Thus, possibly long FAF lifetimes in FLIO indicate compromised RPE at an earlier stage in the pathway to atrophy. A grading of RPE changes relevant to autofluorescence was introduced by Rudolf et al.²⁵ and extended by Zanzottera et al.⁶ Although initially intended to describe RPE changes at the rim of GA,⁶⁷ it categorizes similar lesions as we find here, including nonuniformity of pigmentation and morphology, sloughing, intraretinal migration, and loss of RPE. Interestingly, these authors did not find alterations of the histologic autofluorescence in cells with nonuniform pigmentation and morphology, despite an abnormal expression of polarity markers.⁷ This, again, suggests that fluorescence intensity is less sensitive to early RPE alterations than lifetime.

Along with the change of fluorescence lifetime and an emission spectrum shift, cells may alter their properties and function.⁶⁸ A current immunohistochemistry investigation showed that abnormal RPE lose typical markers like the retinoid isomerohydrolase RPE65. On the other hand, they may gain properties of immune cells, as shown by immunoreactivity for macrophage markers CD68 and CD163.^{43,69} Thus, HRF have been considered macrophages or microglia that phagocytosed RPE.^{70,71} However, HRF can survive for years in the retina and the distribution of granules was found to be preserved in histology.⁶ Therefore, a transdifferentiation of the RPE cells has to be considered.⁵ This transdifferentiation may be associated to the switch of fluorescence properties, however, the mechanism as well as contributing fluorophores still have to be determined.

Although FLIO primarily measures FAF lifetimes, the use of two spectral channels also enables a rough estimation of spectral FAF emission characteristics. This links RPE pathology to hypsochromic shift. Similarly, Marmorstein et al. found a shorter emission maximum for AMD than for control RPE in histology, however, for an excitation wavelength of 364 nm.⁷² Three different spectra were revealed for lipofuscin and melanolipofuscin.⁷³ Hyperspectral FAF imaging in RPE/choroid flatmounts of AMD donor eyes found the same spectra,¹⁹ however, it remains to be determined, whether the relative abundance of related fluorophores changes with RPE pathology as our data suggest. The existence of different fluorophore components, which can be distinguished by their spectra, supports our hypothesis that the fluorophore composition changes in the process of RPE activation and migration.

The following limitations of the current investigation have to be mentioned. This is a retrospective study of clinic patients. Thus, only some patients have follow-up data, and the follow-up intervals were not uniform. That limits our ability to draw conclusions on the progression timeline. This retrospective study also includes patients with varying quality of OCT. Therefore, a number of RPE lesions could not be classified unambiguously, and they were excluded from the analysis. Patients with phakia as well as pseudophakia were included. Although the confocal principle of the Spectralis scanner greatly eliminates fluorescence of the natural lens, it cannot be excluded completely and thus may have biased the fluorescence lifetimes. We minimized the influence of lens autofluorescence by considering the differences of lifetimes and ESIR, respectively, at the RPE lesions and their vicinity (see Table 2). Finally, as a noninvasive clinical imaging technique, FLIO cannot elucidate the chemical nature of the fluorophores exhibiting altered fluorescence lifetimes and emission spectra seen in this study. This clearly limits conclusions on mechanisms of RPE dysmorphia.

In conclusion, we showed that thickening of RPE, hyperpigmentation, and formation of HRF is associated with specific changes in FAF, linking FAF to known progression indicators associated with soft drusen. Whereas initial activation of cells atop drusenoid PED is associated with a shortening of FAF lifetimes in SSC, a switch to long lifetimes was seen after cells sloughed from the intact layer or migrated anteriorly. Thus, FLIO might be used as an early indicator of RPE changes finally leading to atrophy. It should be used in conjunction with OCT to determine the status of RPE health and can be used to study eye-tracked cellular changes that might indicate a risk for AMD progression.

Acknowledgments

Supported by National Institutes of Health (NIH) Grant 1R01EY027948.

Disclosure: **M. Hammer**, None; **J. Jakob-Girbig**, None; **L. Schwanengel**, None; **C.A. Curcio**, None; **S. Hasan**, None; **D. Meller**, None; **R. Schultz**, None

References

1. Sadda SR, Guymer R, Holz FG, et al. Consensus Definition for Atrophy Associated with Age-Related Macular Degeneration on OCT: Classification of Atrophy Report 3. *Ophthalmology*. 2018;125:537-548.

2. Klein R, Klein BE, Knudtson MD, Meuer SM, Swift M, Gangnon RE. Fifteen-year cumulative incidence of age-related macular degeneration: the Beaver Dam Eye Study. *Ophthalmology*. 2007;114:253–262.
3. Klein R, Klein BE, Tomany SC, Moss SE. Ten-year incidence of age-related maculopathy and smoking and drinking: the Beaver Dam Eye Study. *Am J Epidemiol*. 2002;156:589–598.
4. Klein ML, Ferris FL, 3rd, Armstrong J, et al. Retinal precursors and the development of geographic atrophy in age-related macular degeneration. *Ophthalmology*. 2008;115:1026–1031.
5. Curcio CA, Zanzottera EC, Ach T, Balaratnasingam C, Freund KB. Activated Retinal Pigment Epithelium, an Optical Coherence Tomography Biomarker for Progression in Age-Related Macular Degeneration. *Invest Ophthalmol Vis Sci*. 2017;58: BIO211–BIO226.
6. Zanzottera EC, Messinger JD, Ach T, Smith RT, Freund KB, Curcio CA. The Project MACULA Retinal Pigment Epithelium Grading System for Histology and Optical Coherence Tomography in Age-Related Macular Degeneration. *Invest Ophthalmol Vis Sci*. 2015;56:3253–3268.
7. Vogt SD, Curcio CA, Wang L, et al. Retinal pigment epithelial expression of complement regulator CD46 is altered early in the course of geographic atrophy. *Exp Eye Res*. 2011;93:413–423.
8. Ho J, Witkin AJ, Liu J, et al. Documentation of intraretinal retinal pigment epithelium migration via high-speed ultrahigh-resolution optical coherence tomography. *Ophthalmology*. 2011;118:687–693.
9. Zacks DN, Johnson MW. Transretinal pigment migration: an optical coherence tomographic study. *Arch Ophthalmol*. 2004;122:406–408.
10. Miura M, Makita S, Sugiyama S, et al. Evaluation of intraretinal migration of retinal pigment epithelial cells in age-related macular degeneration using polarimetric imaging. *Sci Rep*. 2017;7:3150.
11. Nassisi M, Lei J, Abdelfattah NS, et al. OCT Risk Factors for Development of Late Age-Related Macular Degeneration in the Fellow Eyes of Patients Enrolled in the HARBOR Study. *Ophthalmology*. 2019;126:1667–1674.
12. Spaide RF. Fundus autofluorescence and age-related macular degeneration. *Ophthalmology*. 2003;110:392–399.
13. Schmitz-Valckenberg S, Holz FG, Bird AC, Spaide RF. Fundus autofluorescence imaging: review and perspectives. *Retina*. 2008;28:385–409.
14. Lois N, Owens SL, Coco R, Hopkins J, Fitzke FW, Bird AC. Fundus autofluorescence in patients with age-related macular degeneration and high risk of visual loss. *Am J Ophthalmol*. 2002;133:341–349.
15. Hwang JC, Chan JW, Chang S, Smith RT. Predictive value of fundus autofluorescence for development of geographic atrophy in age-related macular degeneration. *Invest Ophthalmol Vis Sci*. 2006;47:2655–2661.
16. Einbock W, Moessner A, Schnurrbusch UE, Holz FG, Wolf S. Changes in fundus autofluorescence in patients with age-related maculopathy. Correlation to visual function: a prospective study. *Graefes Arch Clin Exp Ophthalmol*. 2005;243:300–305.
17. Bindewald A, Bird AC, Dandekar SS, et al. Classification of fundus autofluorescence patterns in early age-related macular disease. *Invest Ophthalmol Vis Sci*. 2005;46:3309–3314.
18. Ach T, Tolstik E, Messinger JD, Zarubina AV, Heintzmann R, Curcio CA. Lipofuscin redistribution and loss accompanied by cytoskeletal stress in retinal pigment epithelium of eyes with age-related macular degeneration. *Invest Ophthalmol Vis Sci*. 2015;56:3242–3252.
19. Tong Y, Ben Ami T, Hong S, et al. Hyperspectral Autofluorescence Imaging of Drusen and Retinal Pigment Epithelium in Donor Eyes with Age-Related Macular Degeneration. *Retina*. 2016;36(Suppl 1):S127–S136.
20. Holz FG, Bindewald-Wittich A, Fleckenstein M, Dreyhaupt J, Scholl HP, Schmitz-Valckenberg S. Progression of geographic atrophy and impact of fundus autofluorescence patterns in age-related macular degeneration. *Am J Ophthalmol*. 2007;143:463–472.
21. Schmitz-Valckenberg S, Bindewald-Wittich A, Dolar-Szczasny J, et al. Correlation between the area of increased autofluorescence surrounding geographic atrophy and disease progression in patients with AMD. *Invest Ophthalmol Vis Sci*. 2006;47:2648–2654.
22. Schmitz-Valckenberg S, Bultmann S, Dreyhaupt J, Bindewald A, Holz FG, Rohrschneider K. Fundus autofluorescence and fundus perimetry in the junctional zone of geographic atrophy in patients with age-related macular degeneration. *Invest Ophthalmol Vis Sci*. 2004;45:4470–4476.
23. Schmitz-Valckenberg S, Fleckenstein M, Gobel AP, Hohman TC, Holz FG. Optical coherence tomography and autofluorescence findings in areas with geographic atrophy due to age-related macular degeneration. *Invest Ophthalmol Vis Sci*. 2011;52:1–6.
24. Schmitz-Valckenberg S, Fleckenstein M, Scholl HP, Holz FG. Fundus autofluorescence and progression of age-related macular degeneration. *Surv Ophthalmol*. 2009;54:96–117.
25. Rudolf M, Vogt SD, Curcio CA, et al. Histologic basis of variations in retinal pigment epithelium autofluorescence in eyes with geographic atrophy. *Ophthalmology*. 2013;120:821–828.
26. Dysli C, Wolf S, Berezin MY, Sauer L, Hammer M, Zinkernagel MS. Fluorescence lifetime imaging ophthalmoscopy. *Prog Retin Eye Res*. 2017;60:120–143.
27. Sauer L, Andersen KM, Dysli C, Zinkernagel MS, Bernstein PS, Hammer M. Review of clinical approaches in fluorescence lifetime imaging ophthalmoscopy. *J Biomed Opt*. 2018;23:1–20.
28. Sauer L, Vitale AS, Modersitzki NK, Bernstein PS. Fluorescence lifetime imaging ophthalmoscopy: autofluorescence imaging and beyond. *Eye (Lond)*. 2021;35:93–109.
29. Schweitzer D, Schenke S, Hammer M, et al. Towards metabolic mapping of the human retina. *Microsc Res Tech*. 2007;70:410–419.
30. Sauer L, Gensure RH, Andersen KM, et al. Patterns of Fundus Autofluorescence Lifetimes In Eyes of Individuals With Nonexudative Age-Related Macular Degeneration. *Invest Ophthalmol Vis Sci*. 2018;59:AMD65–AMD77.
31. Dysli C, Fink R, Wolf S, Zinkernagel MS. Fluorescence Lifetimes of Drusen in Age-Related Macular Degeneration. *Invest Ophthalmol Vis Sci*. 2017;58:4856–4862.
32. Schultz R, Hasan S, Schwanengel LS, Hammer M. Fluorescence lifetimes increase over time in age-related macular degeneration [published online ahead of print December 20, 2020]. *Acta Ophthalmol*, <https://doi.org/10.1111/aos.14694>.
33. Hammer M, Schultz R, Hasan S, et al. Fundus Autofluorescence Lifetimes and Spectral Features of Soft Drusen and Hyperpigmentation in Age-Related Macular Degeneration. *Transl Vis Sci Technol*. 2020;9:20.
34. Schweitzer D, Hammer M, Schweitzer F, et al. In vivo measurement of time-resolved autofluorescence at the human fundus. *J Biomed Opt*. 2004;9:1214–1222.
35. Sauer L, Schweitzer D, Ramm L, Augsten R, Hammer M, Peters S. Impact of Macular Pigment on Fundus Autofluorescence Lifetimes. *Invest Ophthalmol Vis Sci*. 2015;56:4668–4679.
36. Dysli C, Queller G, Abegg M, et al. Quantitative analysis of fluorescence lifetime measurements of the macula using the fluorescence lifetime imaging ophthalmoscope in healthy subjects. *Invest Ophthalmol Vis Sci*. 2014;55:2106–2113.

37. Klemm M, Schweitzer D, Peters S, Sauer L, Hammer M, Haueisen J. FLIMX: A Software Package to Determine and Analyze the Fluorescence Lifetime in Time-Resolved Fluorescence Data from the Human Eye. *PLoS One*. 2015;10:e0131640.
38. Balaratnasingam C, Yannuzzi LA, Curcio CA, et al. Associations Between Retinal Pigment Epithelium and Drusen Volume Changes During the Lifecycle of Large Drusenoid Pigment Epithelial Detachments. *Invest Ophthalmol Vis Sci*. 2016;57:5479–5489.
39. Sura AA, Chen L, Messinger JD, et al. Measuring the Contributions of Basal Lamina Deposit and Bruch's Membrane in Age-Related Macular Degeneration. *Invest Ophthalmol Vis Sci*. 2020;61:19.
40. Balaratnasingam C, Messinger JD, Sloan KR, Yannuzzi LA, Freund KB, Curcio CA. Histologic and Optical Coherence Tomographic Correlates in Drusenoid Pigment Epithelium Detachment in Age-Related Macular Degeneration. *Ophthalmology*. 2017;124:644–656.
41. Pang CE, Messinger JD, Zanzottera EC, Freund KB, Curcio CA. The Onion Sign in Neovascular Age-Related Macular Degeneration Represents Cholesterol Crystals. *Ophthalmology*. 2015;122:2316–2326.
42. Li M, Dolz-Marco R, Messinger JD, et al. Clinicopathologic Correlation of Anti-Vascular Endothelial Growth Factor-Treated Type 3 Neovascularization in Age-Related Macular Degeneration. *Ophthalmology*. 2018;125:276–287.
43. Cao D, Leong B, Messinger JD, et al. Hyperreflective foci, OCT progression indicators in age-related macular degeneration, include transdifferentiated retinal pigment epithelium. *Invest Ophthalmol Vis Sci*. 2021; under review, preprint available: <https://www.medrxiv.org/content/10.1101/2021.04.26.21256056v2>.
44. Cukras C, Agron E, Klein ML, et al. Natural history of drusenoid pigment epithelial detachment in age-related macular degeneration: Age-Related Eye Disease Study Report No. 28. *Ophthalmology*. 2010;117:489–499.
45. Echols BS, Clark ME, Swain TA, et al. Hyperreflective Foci and Specks Are Associated with Delayed Rod-Mediated Dark Adaptation in Nonneovascular Age-Related Macular Degeneration. *Ophthalmology Retina*. 2020;4:1059–1068.
46. Ferris FL, 3rd, Wilkinson CP, Bird A, et al. Clinical classification of age-related macular degeneration. *Ophthalmology*. 2013;120:844–851.
47. Zanzottera EC, Messinger JD, Ach T, Smith RT, Curcio CA. Subducted and melanotic cells in advanced age-related macular degeneration are derived from retinal pigment epithelium. *Invest Ophthalmol Vis Sci*. 2015;56:3269–3278.
48. Chen KC, Jung JJ, Curcio CA, et al. Intraretinal Hyperreflective Foci in Acquired Vitelliform Lesions of the Macula: Clinical and Histologic Study. *Am J Ophthalmol*. 2016;164:89–98.
49. Chen L, Miyamura N, Ninomiya Y, Handa JT. Distribution of the collagen IV isoforms in human Bruch's membrane. *Br J Ophthalmol*. 2003;87:212–215.
50. Sauer L, Komanski CB, Vitale AS, Hansen ED, Bernstein PS. Fluorescence Lifetime Imaging Ophthalmoscopy (FLIO) in Eyes With Pigment Epithelial Detachments Due to Age-Related Macular Degeneration. *Invest Ophthalmol Vis Sci*. 2019;60:3054–3063.
51. Eldred GE, Katz ML. Fluorophores of the human retinal pigment epithelium: Separation and spectral characterization. *Exp Eye Res*. 1988;47:71–86.
52. Sparrow JR, Parish CA, Hashimoto M, Nakanishi K. A2E, a lipofuscin fluorophore, in human retinal pigmented epithelial cells in culture. *Invest Ophthalmol Vis Sci*. 1999;40:2988–2995.
53. Hammer M, Schultz R, Hasan S, et al. Fundus Autofluorescence Lifetimes and Spectral Features of Soft Drusen and Hyperpigmentation in Age-Related Macular Degeneration. *Transl Vis Sci Technol*. 2020;9:20.
54. Schultz R, Hasan S, Curcio C, Smith RT, Meller D, Hammer M. Spectral and lifetime resolution of fundus autofluorescence in advanced age-related macular degeneration [published online ahead of print July 13, 2021]. *Acta Ophthalmol*, <https://doi.org/10.1111/aos.14963>.
55. Schultz R, Gamage KCLK, Messinger JD, Curcio CA, Hammer M. Fluorescence Lifetimes and Spectra of RPE and Sub-RPE Deposits in Histology of Control and AMD Eyes. *Invest Ophthalmol Vis Sci*. 2020;61:9.
56. Biesemeier A, Taubitz T, Julien S, Yoeruek E, Schraermeyer U. Choriocapillaris breakdown precedes retinal degeneration in age-related macular degeneration. *Neurobiol Aging*. 2014;35:2562–2573.
57. Lipecz A, Miller L, Kovacs I, et al. Microvascular contributions to age-related macular degeneration (AMD): from mechanisms of choriocapillaris aging to novel interventions. *Geroscience*. 2019;41:813–845.
58. Christenbury JG, Folgar FA, O'Connell RV, et al. Progression of Intermediate Age-related Macular Degeneration with Proliferation and Inner Retinal Migration of Hyperreflective Foci. *Ophthalmology*. 2013;120:1038–1045.
59. Giannakaki-Zimmermann H, Querques G, Munch IC, et al. Atypical retinal pigment epithelial defects with retained photoreceptor layers: a so far disregarded finding in age related macular degeneration. *BMC Ophthalmol*. 2017;17:67.
60. Ouyang Y, Heussen FM, Hariri A, Keane PA, Sadda SR. Optical coherence tomography-based observation of the natural history of drusenoid lesion in eyes with dry age-related macular degeneration. *Ophthalmology*. 2013;120:2656–2665.
61. Leuschen JN, Schuman SG, Winter KP, et al. Spectral-domain optical coherence tomography characteristics of intermediate age-related macular degeneration. *Ophthalmology*. 2013;120:140–150.
62. Folgar FA, Chow JH, Farsiu S, et al. Spatial correlation between hyperpigmentary changes on color fundus photography and hyperreflective foci on SDOCT in intermediate AMD. *Invest Ophthalmol Vis Sci*. 2012;53:4626–4633.
63. Kanow MA, Giarmarco MM, Jankowski CS, et al. Biochemical adaptations of the retina and retinal pigment epithelium support a metabolic ecosystem in the vertebrate eye. *Elife*. 2017;6:e28899.
64. Zanzottera EC, Ach T, Huisinck C, Messinger JD, Freund KB, Curcio CA. Visualizing Retinal Pigment Epithelium Phenotypes in the Transition to Atrophy in Neovascular Age-Related Macular Degeneration. *Retina J Ret Vit Dis*. 2016;36:S26–S39.
65. Bermond K, Wobbe C, Tarau IS, et al. Autofluorescent Granules of the Human Retinal Pigment Epithelium: Phenotypes, Intracellular Distribution, and Age-Related Topography. *Invest Ophthalmol Vis Sci*. 2020;61:35.
66. Gamilbril JA, Sloan KR, Swain TA, et al. Quantifying Retinal Pigment Epithelium Dysmorphia and Loss of Histologic Autofluorescence in Age-Related Macular Degeneration. *Invest Ophthalmol Vis Sci*. 2019;60:2481–2493.
67. Waldstein SM, Vogl WD, Bogunovic H, Sadeghipour A, Riedl S, Schmidt-Erfurth U. Characterization of Drusen and Hyperreflective Foci as Biomarkers for Disease Progression in Age-Related Macular Degeneration Using Artificial Intelligence in Optical Coherence Tomography. *JAMA Ophthalmol*. 2020;138:740–747.
68. Jakobiec FA, Barrantes PC, Yonekawa Y, Lad EM, Proia AD. Subretinal Mononuclear Cells in Coats' Disease Studied with RPE65 and CD163: Evidence for Histiocytoid Pigment Epithelial Cells. *Am J Ophthalmol*. 2021;222:388–396.
69. Lad EM, Cousins SW, Van Arnem JS, Proia AD. Abundance of infiltrating CD163+ cells in the retina of postmortem eyes

- with dry and neovascular age-related macular degeneration. *Graefes Arch Clin Exp Ophthalmol*. 2015;253:1941–1945.
70. Lad EM, Cousins SW, Proia AD. Identity of pigmented subretinal cells in age-related macular degeneration. *Graef Arch Clin Exp*. 2016;254:1239–1241.
71. Fleckenstein M, Schmitz-Valckenberg S, Adrion C, et al. Tracking progression with spectral-domain optical coherence tomography in geographic atrophy caused by age-related macular degeneration. *Invest Ophthalmol Vis Sci*. 2010;51:3846–3852.
72. Marmorstein AD, Marmorstein LY, Sakaguchi H, Hollyfield JG. Spectral profiling of autofluorescence associated with lipofuscin, Bruch's Membrane, and sub-RPE deposits in normal and AMD eyes. *Invest Ophthalmol Vis Sci*. 2002;43:2435–2441.
73. Ben Ami T, Tong Y, Bhuiyan A, et al. Spatial and Spectral Characterization of Human Retinal Pigment Epithelium Fluorophore Families by Ex Vivo Hyperspectral Autofluorescence Imaging. *Transl Vis Sci Technol*. 2016;5:5.